Efficiency Evaluation of the Unconditional Maximum Likelihood Estimator for Near-Field DOA Estimation

J. G. Arceo-Olague, D. H. Covarrubias-Rosales, and J. M. Luna-Rivera

In this paper, we address the problem of closely spaced source localization using sensor array processing. In particular, the performance efficiency (measured in terms of the root mean square error) of the unconditional maximum likelihood (UML) algorithm for estimating the direction of arrival (DOA) of near-field sources is evaluated. Four parameters are considered in this evaluation: angular separation among sources, signal-to-noise ratio (SNR), number of snapshots, and number of sources (multiple sources). Simulations are conducted to illustrate the UML performance to compute the DOA of sources in the near-field. Finally, results are also presented that compare the performance of the UML DOA estimator with the existing multiple signal classification approach. The results show the capability of the UML estimator for estimating the DOA when the angular separation is taken into account as a critical parameter. These results are consistent in both low SNR and multiple-source scenarios.

Keywords: Near-field source localization, DOA, UML estimator, sensor array.

I. Introduction

In recent years, source localization using array signal processing has captured the attention of the research community because of its important applications in radar, sonar, wireless systems, seismology, and so on. A basic source localization problem is that of direction of arrival (DOA) estimation for narrowband signals. A wide variety of techniques has already been proposed for the DOA estimation of narrowband sources using an array of sensors [1]. Most of these techniques, however, assume that sources locate relatively far from the array, and thus the wavefronts from the sources can be regarded as plane waves. As the sources approach the array, this assumption is no longer valid. When a source is located close to an array of sensors (near-field), the wavefront of the received signal is curved, and the curvature depends on the distance. Therefore, both the angle and range become parameters of interest.

Early work in DOA estimation includes the early version of the maximum-likelihood (ML) solution [1], but it did not become popular due to its high computational cost [2], [3]. A variety of suboptimal techniques with reduced computations include the minimum variance method of Capon [4], the multiple signal classification (MUSIC) method [5], [6], and high-order subspace-based methods [7], among others. The MUSIC method and Capon's method present, for example, the capability to resolve sources given a moderate signal-to-noise ratio (SNR) value and a sufficient number of data snapshots. These subspace methods provide the advantage of low computational complexity. Although the ML estimator requires a high computational effort due to its likelihood maximization function, it also presents a number of attractive properties which are suitable to the near-field source localization problem. Some

Manuscript received Jan. 11, 2006; revised Aug. 19, 2006.

J. G. Arceo-Olague (phone: + 52 664 623 1344, email: arceojg@citedi.mx) is with Department of Electronics, CITEDI-IPN Research Center, Baja California, Mexico.

D. H. Covarrubias-Rosales (phone: + 52 646 175 0500, email: dacoro@cicese.mx) is with Electronics and Telecommunication Department, CICESE Research Centre, Baja California, Mexico.

J. M. Luna-Rivera (email: mlr@fciencias.uaslp.mx) is with Electronics Department, College of Sciences, UASLP, San Luis Potosi, Mexico.

of these properties are, for instance, consistency, asymptotic unbiasedness, and asymptotic minimum variance [8], [9]. A further important property of ML-based techniques is that they provide resolvability of closely-spaced sources in the presence of high levels of noise. To reduce the complexity of the ML estimator, several suboptimal methods have been proposed such as the genetic algorithms in [11], the alternating projection scheme [10], the expectation/maximization (EM) iterative method [12], and the conditional ML [13]. An estimator of particular interest is the conditional ML which considers unknown but deterministic signals. However, if a random type of signal is considered, it is required to incorporate the statistics of this signal. Such statistics are considered by the unconditional maximum likelihood (UML) estimator [8] which we will focus on this paper. In [8], the problem of calculating maximum likelihood estimates through a close-form solution is overcome by employing the iterative EM algorithm.

The authors of [6] have shown that DOA estimation efficiency can be improved when angular separation between two sources is introduced. However, a compromise between SNR values and the number of data snapshots must be accomplished in order to improve the resolution in the DOA estimation. It has also been shown that the performance of DOA estimation algorithms may be significantly affected by variations in these parameters. In this paper, we evaluate the performance efficiency of the UML method for estimating the DOA of narrowband sources in the near-field using a uniform array of sensors. The performance, in terms of the root mean square, of the UML estimator is evaluated as a function of angular separation, SNR and snapshots between signal sources. Furthermore, the performance of the UML estimator is also considered for the multiple sources environment. The experimental analysis on simulated data demonstrates that the UML estimator offers increased resolution, robustness to noise, and improvements in data quantity, as compared to methods such as MUSIC. The MUSIC algorithm is perhaps one of the most popular suboptimal techniques. Therefore, we establish a comparison with this algorithm under the same circumstances.

The paper is organized as follows. Section II defines the notations used in this paper. Section III introduces the signal model of interest. Section IV summarizes the key points in the derivation of the UML as well as the main steps of the iterative EM algorithm. In section V, a series of computer simulations are presented to demonstrate the improved performance of the UML estimator. Finally, we draw some conclusions in section VI.

II. Nomenclature

- $(.)^{T}$: matrix transpose.
- $(.)^{H}$: matrix conjugate transpose.
- $\boldsymbol{\mu}=[\mu_1,\cdots,\mu_d] \in \Re^{d\times 1}$: far-field vector.
- $\boldsymbol{\zeta}=[\zeta_1,\cdots,\zeta_d] \in \Re^{d\times 1}$: near-field vector.
- $\mathbf{s}\in\Im^{d\times 1}$: signal vector.
- $\mathbf{x}(t_n)=[x_{kmin},\cdots,x_{kmax}] \in \Im^{M\times 1}$: outgoing vector of the array at time t_n.
- $\mathbf{A}\{\boldsymbol{\mu}, \boldsymbol{\zeta}\}=[\mathbf{a}(\mu_1, \zeta_1),\cdots, \mathbf{a}(\mu_d, \zeta_d)] \in \Im^{M\times d}$: array steering matrix.
- $\mathbf{X}=[\mathbf{x}^{T}(1),\cdots,\mathbf{x}^{T}(N)]^{T} \in \Im^{M\times N}$: outgoing matrix for N samples.

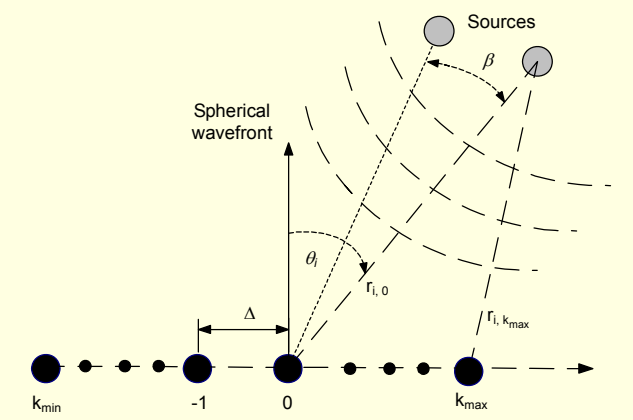

Fig. 1. Narrowband sources in the near-field impinging on a uniform array of sensors.

III. Signal Modelling

Consider the narrowband model for near-field sources impinging upon a linear array of M omnidirectional sensors ($k\in K=\{k_{min},\cdots, k_{max}\}$) as shown in Fig. 1. Due to non-uniform spatial loss in the near-field geometry, the signal strength at each sensor can be different. Therefore, every element has a gain which in this case is normalised to 1.

The sensor array elements are assumed to be uniformly separated by a distance $\Delta=\lambda/4$, where λ denotes the wavelength. The variable β defines the separation between two sources. Let $s_i(t_n)$, and $\boldsymbol{\theta}_i=[\theta_1,\cdots,\theta_i]$, i=1, 2,⋯,d, be the complex envelope and a sampling grid of all directions of arrival for d sources respectively; then the observation model at the output of the k-th array element for the t_n sample can be expressed as

$$x_k(t_n)=\sum_{i=1}^{d} s_i(t_n)\, e^{j(\mu_i k+\zeta_i k^2)}+n_k(t_n),\ 1\le t_n\le N \qquad (1)$$

where the first component of the phase, $(\mu_i k)$ with $\mu_i=-(2\pi\Delta/\lambda)\sin\theta_i$, corresponds to the phase contribution in the far-field, and the second term, $\zeta_i=-(2\pi\Delta^2/\lambda r_i)\cos^2\theta_i$, is a second-order polynomial which is used to approximate the spherical wavefront effect of the source in the near-field [8]. The non-

linear function ζ_i incorporates the distance effect between each source and the k-th sensor array r_i, and the azimuth θ_i into the observation model. Taking a sample from each sensor, we can use (1) to express in a matrix form the observed signal for the sensor array. Thus the M×1 array output signal, $\mathbf{x}(t_n)=[x_{kmin}(t_n),\cdots, x_k(t_n),\cdots, x_{kmax}(t_n)]^T$, can be expressed as

$$\mathbf{x}(t_n) = \mathbf{A}(\mu,\xi)\mathbf{s}(t_n) + \mathbf{n}(t_n), \quad 1 \le t_n \le N \tag{2}$$

where the d×1 vector $\mathbf{s}(t_n)=[s_1(t_n),\cdots, s_d(t_n)]^T$ groups the source signal and the M×1 vector $\mathbf{n}(t_n)=[n_{kmin}(t_n),\cdots,n_k(t_n),\cdots, n_{kmax}(t_n)]^T$, the noise samples corresponding to the M output sensor signals. The matrix $\mathbf{A}(\boldsymbol{\mu}, \boldsymbol{\zeta})$ denotes the steering matrix of dimensions M×d where the i-th column is defined by

$$\mathbf{a}(\mu_i,\zeta_i) = \begin{bmatrix} e^{j(k_{\min}\mu_i + k_{\min}^2\zeta_i)} \\ \vdots \\ 1 \\ e^{j(\mu_i+\zeta_i)} \\ e^{j(2\mu_i+4\zeta_i)} \\ \vdots \\ e^{j(k_{\max}\mu_i + k_{\max}^2\zeta_i)} \end{bmatrix}. \tag{3}$$

Considering variations in the SNR values, and given a small angle separation β among sources, this paper is mainly concerned with determining the UML estimator efficiency for DOA estimation of sources in the near-field. In this paper, efficiency will be evaluated in terms of the root mean square error (RMSE). In the next section, we review the main points in the derivation of the UML estimator.

IV. UML Estimator

In this section, we summarise the derivation of the UML estimator for the near-field source localization problem stated in this paper. The UML estimator was originally addressed in [8]. In order to derive the UML estimator, the following assumptions are made on the signal modelling process. First, it is assumed that the source signal, $\boldsymbol{s}(t_n)$, and the noise, $\boldsymbol{n}(t_n)$, are temporally and spatially uncorrelated zero-mean complex Gaussian random processes. Therefore, it can be shown that the covariance matrix for the observed data vector $\boldsymbol{X}$ can be defined as

$$\begin{aligned} \mathbf{K}_x(\mu,\zeta,\mathrm{K}_s) &= E[\mathbf{x}(t_n)\mathbf{x}^H(t_m)] \\ &= \mathbf{A}(\mu,\zeta)\mathbf{K}_s\mathbf{A}^H(\mu,\zeta) + \sigma^2\mathbf{I}, \end{aligned} \tag{4}$$

where $\mathbf{K}_s$ is the unknown covariance matrix of the uncorrelated source signals, that is, $\mathbf{K}_s$ =diag[$\alpha_1,\cdots,\alpha_i,\cdots,\alpha_d$] (with α_i as its coefficients), and σ^2 is the noise variance which is assumed to be known. Thus the joint probability density function of the observation vector $\boldsymbol{X}$, given $\{\boldsymbol{\mu}, \boldsymbol{\zeta}, \mathbf{K}_s\}$, can be described by

$$f(\mathbf{X};\boldsymbol{\mu},\boldsymbol{\zeta},\mathbf{K}_s) = \prod_{t_n=1}^{N} \pi^{-M} \det(\mathbf{K}_x)^{-1} \times \exp(-\mathbf{x}^H(t_n)\mathbf{K}_x^{-1}\mathbf{x}(t_n)). \tag{5}$$

In order to yield the measure of uncertainty, the negative log-likelihood function is considered. Using (5), and after some simplifications, the resulted objective function is given by

$$L(x;\boldsymbol{\mu},\boldsymbol{\zeta},\mathbf{K}_s) = -\ln\det(\mathbf{K}_x) - \frac{1}{N} tr\left[\mathbf{K}_x^{-1}\sum_{t_n=1}^{N}\mathbf{x}(t_n)\mathbf{x}^H(t_n)\right]. \tag{6}$$

Furthermore, given the fact that $\mathbf{x}(t_n)$ is second-order ergodic [8], we find that

$$\mathbf{K}_x = \lim_{N\to\infty}\hat{\mathbf{K}}_x = \lim_{N\to\infty}\frac{1}{N}\sum_{t_n=1}^{N}\mathbf{x}(t_n)\mathbf{x}^H(t_n), \tag{7}$$

where $\hat{\mathbf{K}}_x$ is the sampling covariance matrix. Therefore, the negative log-likelihood function can now be represented as

$$L(x;\boldsymbol{\mu},\boldsymbol{\zeta},\mathbf{K}_s) = -\ln\det(\mathbf{K}_x) - tr[\mathbf{K}_x^{-1}\mathbf{K}_x]. \tag{8}$$

Minimizing the negative of a log-likelihood function thus produces maximum likelihood estimates. However, the minimization problem of the objective function in (8) turns out to be a problem where finding a unique solution through a closed-form formula is not possible [8], [12]; therefore, an alternative solution to this optimization problem is the application of a numerical solution. To solve this minimization problem, the computationally efficient iterative solution called the EM algorithm has been proposed by Cekli and Cirpan in [8]. This algorithm decomposes the observed data into its signal components and then yields an estimate of each source component separately. A brief review of the EM algorithm is presented next.

EM Algorithm

In order to apply the EM algorithm, it is necessary to define a complete set of data associated with the negative log-likelihood objective function given in (8). The EM algorithm approximates the ML estimate in an iterative fashion. However, this iterative process can be simplified by choosing an appropriate log-likelihood function of the complete data so that this function can be easily estimated and maximized from the

incomplete data. Therefore, a particular choice for the complete data can be given by

$$\mathbf{y}_l(t_n) = \mathbf{a}(\mu_l, \zeta_l) s_l(t_n) + \mathbf{n}_l(t_n), \quad 1 \le l \le d \tag{9}$$

where $\mathbf{n}_l(t_n)$ is the Gaussian noise vector corresponding to the l-th signal, that is

$$\mathbf{n}_l(t_n) = \frac{1}{d}[\mathbf{x}(t_n) - \mathbf{A}(\boldsymbol{\mu}, \boldsymbol{\zeta})\mathbf{s}(t_n)], \quad 1 \le l \le d\ . \tag{10}$$

For the set of N samples and d sources, it is necessary to establish the relation between the set of complete data and the incomplete data. In this case, this relationship is given by

$$\mathbf{x}(t_n) = \sum_{l=1}^{d} \mathbf{y}_l(t_n), \quad 1 \le t_n \le N\ . \tag{11}$$

In (11), the complete data $\mathbf{y}_l(t_n)$ is observed as a Gaussian process with mean zero and covariance $\mathbf{K}_y$. Then the log-likelihood function of $\mathbf{y}_l(t_n)$ is evaluated as

$$L(\mathrm{y}_l; \boldsymbol{\mu}, \boldsymbol{\zeta}, \mathbf{K}_s) = -\ln \det(\mathbf{K}_{y_l}) - tr[\mathbf{K}_{y_l}^{-1}\hat{\mathbf{K}}_{y_l}]. \tag{12}$$

In this way, the EM algorithm optimises the log-likelihood function of the complete data. The expectation in the EM algorithm involves the conditional expectation of the log-likelihood of the complete data with respect to the previous estimates of $\{\boldsymbol{\mu}^p, \boldsymbol{\zeta}^p, \mathbf{K}_s\}$. On the other hand, the maximization process yields an estimate of the parameters $\{\boldsymbol{\mu}^p, \boldsymbol{\zeta}^p, \mathbf{K}_s\}$. This is achieved by maximizing the log-likelihood function of the complete data. This optimization process is then repeated for each source. An outline of the EM algorithm can be summarized through 3 steps.

Step 1. Initialization

For the first source, set the initial phase and coefficient values $\{\mu_l^0, \zeta_l^0, \alpha_l^0\}$ for p=0.

Step 2. Expectation

Subsequently, for p=p+1 calculate with the following:

1) From the near-field estimated parameters $\{\mu^{p+}, \zeta^{p+}\}$, obtain $\mathbf{K}_{y_l}^p$ and $\mathbf{K}_{x_l}^p$ with

$$\begin{aligned} \mathbf{K}_{\mathbf{x}_1}^p &= \mathbf{A}(\mu^p, \zeta^p)\mathbf{K}_s^p\mathbf{A}^H(\mu^p, \zeta^p) + \sigma^2\mathbf{I} \\ \mathbf{K}_{\mathbf{y}_1}^p &= \alpha_l^p \mathbf{a}(\mu_l, \zeta_l)\mathbf{a}^H(\mu_l, \zeta_l) + \frac{\sigma^2}{d}\mathbf{I} \end{aligned} \tag{13}$$

2) Given (13), estimate $\hat{\mathbf{K}}_{y_1}^{p+1}$

$$\begin{aligned} \mathbf{K}_{\mathbf{y}_1}^{p+1} &= E\{\mathbf{K}_{y_l} \,|\, \mathbf{K}_{\mathbf{y}_1}^p, \mathbf{K}_{\mathbf{x}}^p, \hat{\mathbf{K}}_{\mathbf{x}}\} \\ &= \mathbf{K}_{\mathbf{y}_1}^p (\mathbf{K}_{\mathbf{x}}^p)^{-1}\left[\hat{\mathbf{K}}_{\mathbf{x}}(\mathbf{K}_{\mathbf{x}}^p)^{-1} - \mathbf{I}\right]\mathbf{K}_{\mathbf{y}_1}^p + \mathbf{K}_{\mathbf{y}_1}^p \end{aligned} \tag{14}$$

Step 3. Maximization

Maximize the likelihood function from the complete data with respect to the estimated parameters for $\alpha_l > 0$. To estimate the parameters $\{\mu^{p+1}, \zeta^{p+1}\}$, substitute $\hat{\mathrm{K}}_{y_l}^{p+1}$ in (15).

$$\begin{aligned} \{\mu^{p+1}, \zeta^{p+1}\} &= \arg\max_{\{\mu_l, \zeta_l\}} \frac{\mathbf{a}^H(\mu_l, \zeta_l)\hat{\mathbf{K}}_{y_l}^{p+1}\mathbf{a}(\mu_l, \zeta_l)}{|\mathbf{a}(\mu_l, \zeta_l)|^2} \\ \alpha_l^{p+1} &> 0 \end{aligned} \tag{15}$$

For $\{\mu^{p+1}, \zeta^{p+1}\}$, calculate the coefficient α_l^{p+1} for $\mathbf{K}_s$ as

$$\begin{aligned} \alpha_l^{p+1} = &\frac{1}{\left|\mathbf{a}\left(\mu_l^{p+1}, \zeta_l^{p+1}\right)\right|^2} \\ &\times\left(\frac{\mathbf{a}^H\left(\mu_l^{p+1}, \zeta_l^{p+1}\right)\hat{\mathbf{K}}_{y_l}^{p+1}\mathbf{a}\left(\mu_l^{p+1}, \zeta_l^{p+1}\right)}{\left|\mathbf{a}\left(\mu_l^{p+1}, \zeta_l^{p+1}\right)\right|^2} - \frac{\sigma^2}{d}\right). \end{aligned} \tag{16}$$

The steps 2 and 3 are repeated until $\{\mu_l, \zeta_l\}$ and α_l converge.

Cramer-Rao bounds (CRBs) [8] on the asymptotic performance of near-field source location estimators are valid for providing a lower bound on the error variance of any unbiased estimator. In this paper, we make use of the CRBs as a benchmark for analyzing and comparing the performance efficiency of the UML estimator. As in the Appendix, these asymptotical bounds are defined as

$$CRB^{-1}(\tau) = \frac{2N}{\sigma^2}\mathrm{Re}\left\{\mathrm{A}^H\,\Pi^c\,\mathrm{A} \bullet (\mathbf{1} \otimes \mathrm{K_s}\mathrm{A}^H\,\mathrm{K_x^{-1}}\,\mathrm{AK_s})^T\right\}, \tag{17}$$

where $\mathbf{\Pi}^C = \mathbf{I} - \mathbf{A}\left[\mathbf{A}^H\mathbf{A}\right]^{-1}\mathbf{A}^H$, and $\mathbf{1}$ is a matrix of ones. The operators $\bullet$ and $\otimes$ denote the inner and Kronecker products, respectively. For a complete derivation on these bounds, refer to [8].

V. Simulation Results

To evaluate the performance efficiency of the UML estimator, we obtain and compare the asymptotical and estimated DOA RMSE for closely-spaced near-field sources. Simulation results are mainly presented in terms of the angle separation among the sources, a variable mostly neglected in

the research community when estimating the DOA of near-field sources. These simulations are intended to show the performance efficiency of the UML estimator in undesirable conditions, that is, by increasing the number of sources and low SNR given an angular separation β.

A uniform linear array of M=7 sensors separated by a quarter wavelength (d=λ/4) of the actual narrowband source signals is considered. It implies that the antenna array with its half power beamwidth can resolve two sources when they are separated by an angle β > 14.5. In this section, we report three different experiments which were carried out to show the UML DOA estimator performance. It was assumed that all sources transmit with the same power for all the scenarios considered here. The first two experiments were set up to obtain the DOA RMSE estimations given an angular separation β. These simulations were computed for different SNR values and number of input data snapshots. In the third experiment, the UML DOA estimation performance as a function of SNR was obtained for the scenario of multiple sources. In addition, we applied the MUSIC algorithm and computed the CRB using (17) for comparison purposes.

1. DOA Estimation with Angular Source Separation and SNR Variations

We first consider two narrowband sources in the near-field impinging upon the sensor array. These sources were placed in $\{\theta_1, r_1\}=\{10°, 10\lambda\}$ and $\{\theta_2, r_2\}=\{\theta_1+\beta, 11.8\lambda\}$, respectively, where r_1 and r_2 specify the distances between the sensor array and each of the sources.

Figures 2 and 3 show the relation between the average DOA RMSE estimates and the angular separation β when using the MUSIC and the UML estimators. The number of snapshots was set to 1000 and the SNR varied from 0 dB to 11 dB. A total of 200 independent trials were performed for each simulation.

Figure 2 shows the results obtained using the MUSIC algorithm. It can be observed that the RMSE of the estimated DOA presents a significant performance variation as the angular separation β is increased. For example, the RMSE shows a two-order variation for an SNR of 11 dB, this goes from the range of 25° in β=5° to 0.25° with β=12°. If the SNR is reduced, the variation of the RMSE estimation lessens as well, but this comes at the cost of large values in the RMSE. A further analysis of the plots in Fig. 2 illustrates that if we set up a maximum RMSE value, for instance, to one degree, this performance would be reached only when β≥8 degrees and the SNR is between 9 and 11 dB. These results are useful to illustrate that the MUSIC algorithm degrades significantly when the angular separation β and the SNR are varying. Following a similar analysis of the UML estimator

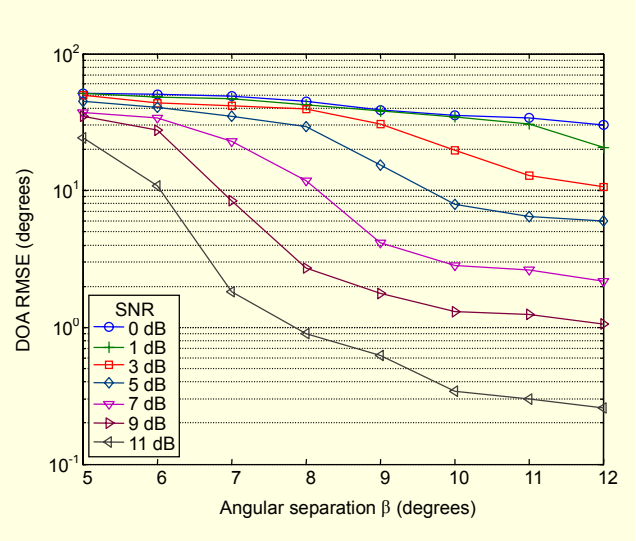

Fig. 2. RMSE of MUSIC estimations for two sources with different separation. Estimation with 1000 samples.

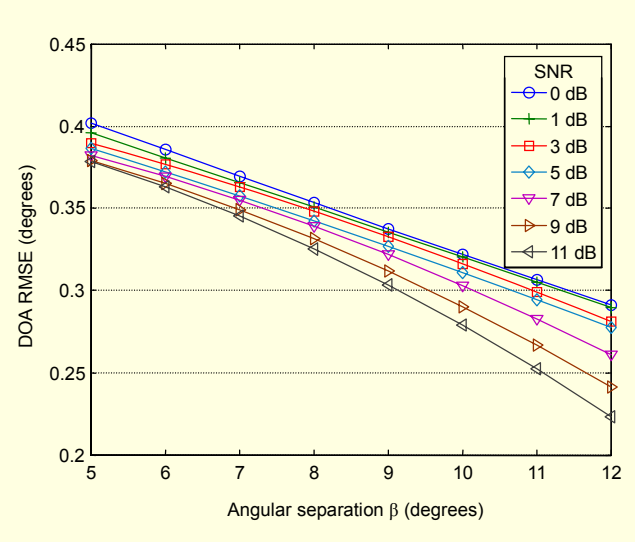

Fig. 3. RMSE of UML estimations for sources with different separations. Estimations with 1000 samples.

performance, which is shown in Fig. 3, it can be seen that only small variations are obtained when varying the angular separation and the SNR. Looking at the plot corresponding to the case of an SNR=0 dB, we observe that the RMSE of the DOA estimates varies from 0.41 to 0.29° corresponding to the cases of β=5° and β=12°, respectively. It is also clear that the UML estimator for higher values of SNR up to 11 dB achieves a similar performance. Notice that due to the small variations of the RMSE values in Fig. 3, we have displayed the vertical axis in a linear scale. One aspect of the UML technique is that it is able to yield estimates with small RMSE values. Figure 3 shows RMSE values within an interval of 0.5 degree. Other

source localization methods have much difficulty resolving closely-spaced sources, especially at low SNR levels; therefore, small RMSE values can be considered a good performance compromise. As compared with the MUSIC algorithm, the UML estimator has improved the performance for low SNR by exhibiting very small variations when the angular separation changes.

2. DOA Estimation with Angular Source Separation and SNR Variations for a Reduced Number of Input Samples

A second set of simulations were carried out with the purpose of evaluating the influence of the number of snapshots while determining the efficiency of the UML estimator for locating a source in the near-field. For these simulations, it was also considered the case of a two-source scenario but only 500 samples were processed, half the number of samples used in the previous experiment.

In Fig. 4, we plotted the RMSE of the DOA estimation using MUSIC as a function of the angular separation between the two sources when the SNR varies from 0 dB to 11 dB. We note that MUSIC is not able to satisfy the consideration of one degree as the maximum DOA RMSE allowed for all values of SNR and β considered in these simulations.

We next show the simulation results using the UML estimator. These results are plotted in Fig. 5. From these results, it is clear to observe that under the two-source scenario, the UML estimator can estimate the sources position within a maximum RMSE of one degree.

As before, the vertical axis in Fig. 5 is set to a linear scale in order to present the results in a clearer fashion. Analyzing Fig. 5, we observe that, for the SNR=0 dB case, the UML estimator

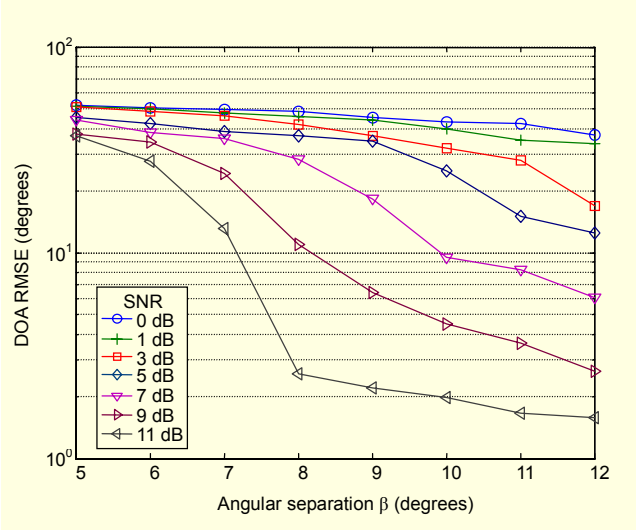

Fig. 4. RMSE of MUSIC estimations for two sources with different separation. Estimation with 500 samples.

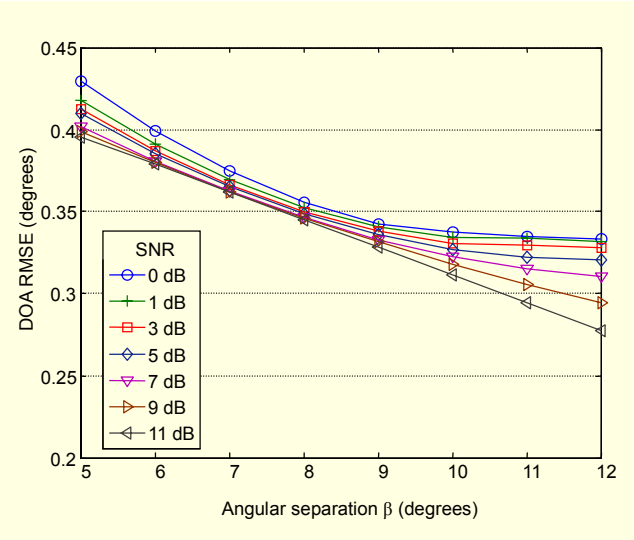

Fig. 5. RMSE of UML estimations for two sources with different separation. Estimation with 500 samples.

manages to estimate the sources' DOA with an RMSE value of 0.45 degrees for all the angular positions considered. Analyzing Fig. 5, we observe that, for the SNR=0 dB case, the UML estimator manages to estimate the sources' DOA with an RMSE value of 0.45 degrees for all the angular positions considered. It is then evident that the performance efficiency of the UML estimator becomes more robust than MUSIC to the effect of reducing the number of input samples when a small angular separation β between sources is considered.

3. DOA Estimation for a Multiple Source Scenario and SNR Variations

Finally, we present the performance evaluation for the UML and MUSIC estimators under the multiple source scenario. In this framework, we consider the existence of 5 sources where the *i*-th source was placed at the location $\{\theta_i, r_i\}$, with $\theta_i \in \{10°, 15°, 20°, 25°, 30°\}$ and $r_i \in \{10\lambda, 11.8\lambda, 10.3\lambda, 11.4\lambda, 9.8\lambda\}$, for $i=1, 2, \cdots, 5$. The total number of snapshots was 1000 and the SNR was 11 dB. Figure 6 shows the performance of the MUSIC algorithm to resolve the 5 closely-spaced sources with a constant angular separation of 5°. In this case, the MUSIC algorithm managed to resolve only three of the sources, failing to estimate the location of the other two.

The estimated sources were at the following locations [38.80°, 5.26°, -42.14°]. From these results we can observe that two of these estimates have an RMSE value lower than 10º while the third estimated source has a far worse estimation accuracy of DOA than the previous two (RMSE higher than 50°). As can be observed in Fig. 6, the DOA accuracy loss is large for the MUSIC algorithm under this multiple source

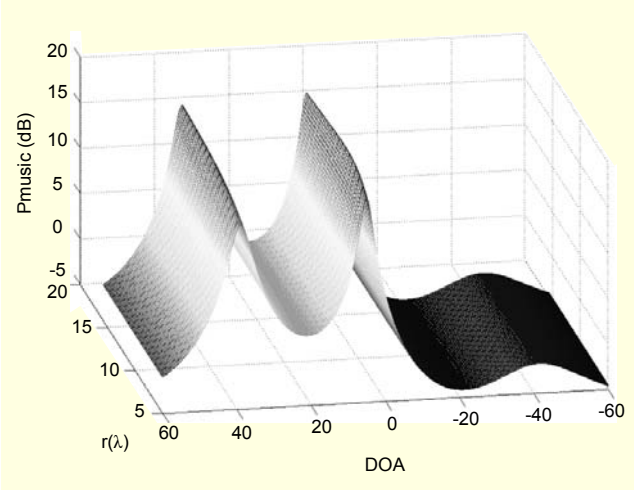

Fig. 6. MUSIC spectrum during the estimation of multiple sources, angular separation 5°. Estimation with 1000 samples.

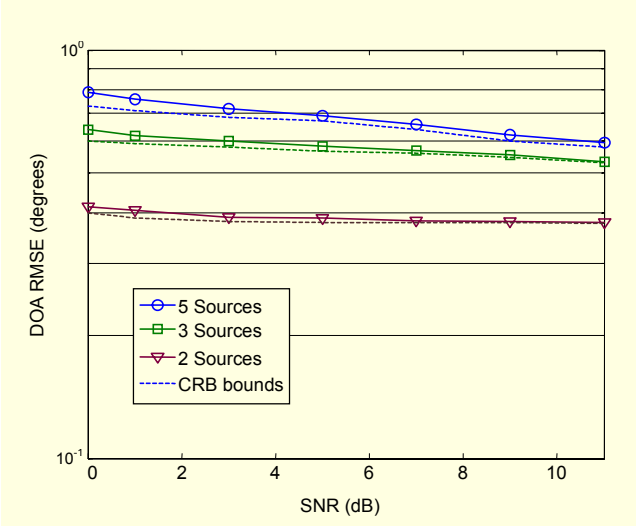

Fig. 7. RMS error of UML during the estimation of multiple sources, angular separation 5°. Estimation with 1000 samples.

scenario. On the other hand, Fig. 7 depicts the performance of the UML estimator for the same scenario. The cases taking the first two sources or the first 3 sources are also included in these simulations. In contrast, the UML estimator shows more satisfactory DOA estimations than MUSIC resulting in the localization of all sources. Recall that the maximum value of RMSE error allowed is one degree. Therefore, the UML estimator can achieve a good accuracy of the source DOA. Changing the number of sources from two to five, the DOA RMSE values computed range from 0.4° to 0.8°; however, the maximum RMSE value allowed is never reached. For each case of DOA estimation, Fig. 7 shows the Cramer-Rao bounds, which are used as a benchmark to compare the results obtained by the UML estimator. We can observe that the UML performance can approach the Cramer-Rao bounds as the SNR is increased, although a small error is perceived when we increase the number of sources.

VI. Conclusions

In this paper we have reported the performance behaviour of the UML estimator under different conditions: 1) low SNR values, 2) angular separation among sources, 3) varying the number of input samples and 4) increasing the number of sources (multiple sources). The experimental results on simulated data demonstrate that the UML estimator exhibits a smaller loss in DOA estimation performance as compared to the MUSIC algorithm under all the conditions considered in this paper. Extensive computer simulations have shown the DOA RMSE performance for the UML estimator under different scenarios. Considering the case of multiple sources, we found that the minimum angular separation among sources was 5º for a SNR of 0 dB. We can conclude that by increasing the number of sources, the UML estimator can still yield good estimates of the DOA sources, making this algorithm a technique which is robust to this environment. Finally, it can be stated that the angular separation β is a critical parameter for the DOA algorithms, even for the UML estimator. This is evident in comparing the small RMSE variations when the SNR and/or number of input samples changes.

Appendix. Cramer-Rao Bounds

The parameter of interest is $\boldsymbol{\tau} = [\boldsymbol{\mu}^T, \boldsymbol{\zeta}^T]^T$. To focus on the parameters of interest requires the concentrated likelihood approach to obtain the CRB [14]. Then the Fisher information matrix (FIM) is given to the (i,j)-th element by

$$\mathbf{J}_{ij}(\boldsymbol{\tau}) = Ntr\left[\mathbf{K}_x^{-1}\left[\frac{\partial \widetilde{\mathbf{K}}_x}{\partial \boldsymbol{\tau}_i}\right]_\infty \mathbf{K}_x^{-1}\left[\frac{\partial \widetilde{\mathbf{K}}_x}{\partial \boldsymbol{\tau}_j}\right]_\infty\right] \tag{A1}$$

The $[]_\infty$ is defined as the almost sure limit of $[\cdot]$, and $\widetilde{\mathbf{K}}_x$ is the concentrated covariance after substituting the ML estimates $\hat{\mathbf{K}}_x$ for $\mathbf{K}_x$ when the limit $N \to \infty$.

Suppressing the dependence of $\mathbf{A}$ on $(\boldsymbol{\mu}, \boldsymbol{\zeta})$ for notational convenience, the concentrated covariance $\hat{\mathbf{K}}_x$ with respect to $\hat{\mathbf{K}}_s \to \hat{\mathbf{K}}_s$ yields

$$\widetilde{\mathbf{K}}_x = \mathbf{A}\hat{\mathbf{K}}_s\mathbf{A}^H + \sigma^2\mathbf{I} = \boldsymbol{\Pi}\hat{\mathbf{K}}_x\boldsymbol{\Pi} + \sigma^2\boldsymbol{\Pi}^c, \tag{A2}$$

where

$$\boldsymbol{\Pi} \triangleq \mathbf{A}[\mathbf{A}^H\mathbf{A}]^{-1}\mathbf{A}^H \quad \text{and} \quad \boldsymbol{\Pi}^c \triangleq \mathbf{I} - \boldsymbol{\Pi}. \tag{A3}$$

Letting $\partial\mathbf{\Pi}/\partial\boldsymbol{\tau}_i$ be denoted by $\mathbf{\Pi}_i$, for any i=1,⋯,2d and taking the limit $N \to \infty$, thus from (A2), the following are immediate:

$$\left(\frac{\partial\widetilde{\mathbf{K}}_x}{\partial\boldsymbol{\tau}_i}\right) = \mathbf{\Pi}_i\mathbf{K}_x\mathbf{\Pi} + \mathbf{\Pi}\mathbf{K}_x\mathbf{\Pi}_i + \sigma^2\mathbf{\Pi}_i^c \quad \text{(A4)}$$

and applying (A1) give

$$\mathbf{J}_{ij}(\boldsymbol{\tau}) = Ntr[\mathbf{K}_x^{-1}(\mathbf{\Pi}_i\mathbf{K}_x\mathbf{\Pi}+\mathbf{\Pi}\mathbf{K}_x\mathbf{\Pi}_i+\sigma^2\mathbf{\Pi}_i^c) \times\mathbf{K}_x^{-1}(\mathbf{\Pi}_j\mathbf{K}_x\mathbf{\Pi}+\mathbf{\Pi}\mathbf{K}_x\mathbf{\Pi}_j+\sigma^2\mathbf{\Pi}_i^c)]. \quad \text{(A5)}$$

Next, we note that

$$\mathbf{\Pi}_i = \mathbf{\Pi}^c\mathbf{A}_i\mathbf{A}^\dagger + (\mathbf{A}^H)^\dagger\mathbf{A}_i^H\mathbf{\Pi}^c$$

where $(.)^\dagger$ is the pseudo inverse (Moore-Penrose inverse).

Evaluating (A5) and then reducing terms gives

$$tr\left(\mathbf{K}_x^{-1}\left[\frac{\partial\widetilde{\mathbf{K}}_x}{\partial\boldsymbol{\tau}_i}\right]_\infty\mathbf{K}_x^{-1}\left[\frac{\partial\widetilde{\mathbf{K}}_x}{\partial\boldsymbol{\tau}_j}\right]_\infty\right) = 2\,\mathrm{Re}\{tr\{\mathbf{A}_I^H\mathbf{\Pi}^c\mathbf{A}_j\times\frac{\mathbf{K}_s}{\sigma^2}-(\mathbf{A}^H\mathbf{A})^{-1}+\sigma^2\mathbf{A}\mathbf{K}_x^{-1}(\mathbf{A})^H\}\}. \quad \text{(A6)}$$

From these results and after reduction, the FIM elements are

$$\mathbf{J}_{ij}(\boldsymbol{\tau}) = \frac{2N}{\sigma^2}\mathrm{Re}\left\{(\mathbf{A}^H\mathbf{\Pi}^c\mathbf{A})_{ij}(\mathbf{1}\otimes\mathbf{K}_s\mathbf{A}^H\mathbf{K}_X^{-1}\mathbf{A}\mathbf{K}_s)_{ji}\right\}$$

Finally, the $\mathrm{CRB}^{-1}(\boldsymbol{\tau})$ matrix derived is as follows:

$$CRB^{-1}(\boldsymbol{\tau}) = \frac{2N}{\sigma^2}\mathrm{Re}\left\{\mathbf{A}^H\mathbf{\Pi}^c\mathbf{A}\bullet(\mathbf{1}\otimes\mathbf{K}_s\mathbf{A}^H\mathbf{K}_x^{-1}\mathbf{A}\mathbf{K}_s)^T\right\}, \quad \text{(A7)}$$

where **1** is defined as a matrix of ones.

References

[1] H. Krim and M. Viber, "Two Decades of Array Signal Processing Research: The Parametric Approach," *IEEE Signal Proc. Mag.* vol. 13, no. 4, July 1996, pp. 67-94.

[2] H.L. Van Trees, *Optimum Array Processing, Part IV*, Wiley-Interscience, Canada, 2002.

[3] D.H. Johnson and D.E. Dudgeon, *Array Signal Processing: Concepts and Techniques*, Prentice Hall, 1993.

[4] J. Capon, "High Resolution Frequency-Wavenumber Spectrum Analysis," *Proc. IEEE*, vol. 57, no. 8, 1969, pp. 1408-1418.

[5] R.O. Schmidt, "Multiple Emitter Location on Signal Parameter Estimation," *IEEE Trans. on Antennas and Propagation*, vol. 34, no. 3, Mar. 1986, pp. 276-280.

[6] D.H. Covarrubias-Rosales and J.G. Arceo Olague, "Improving Resolution on DOA Estimation in a Multipath Macrocell Environment Using Eigenstructure-Based Methods," *Proc. Sympotic 2004*, IEEE Bratislava, Slovak Republic, pp. 39-42.

[7] R.N.Challa and S.Shamsunder, "High-Order Subspace-Based Algorithms for Passive Localization of Near-*Field* Sources," *Proc. 29th Asimolar Conf. on Signals, Systems and Computers*, vol. 2, Nov. 1995, pp. 777-781.

[8] E. Çekli and H.A. Çirpan, "Unconditional Maximum Likelihood Approach for Localization of Near-Field Sources: Analysis and Performance Analysis," *AEÜ Int'l J. of Electron. and Commun.*, vol. 57, no. 1, 2003, pp. 9-15.

[9] S. Kay, *Fundamentals of Statistical Signal Processing: Estimation Theory,* vol. 2, Englewood Cliffs, Prentice Hall, 1993, pp. 157-214.

[10] I. Ziskind and M. Wax, "Maximum Likelihood Localization of Multiple Sources by Alternating Projection," *IEEE Trans. on Acoustics, Speech, and Signal Processing*, vol. 36, no. 10, Oct. 1998, pp 1553-1560.

[11] M.H. Li and Y.L. Lu, "Improving the Performance of GA-ML-DOA Estimator with a Resampling Scheme," *Elsevier-Signal Processing*, vol. 84, Oct. 2004, pp. 1813-1822.

[12] T.K. Moon, "The Expectation-Maximization Algorithm," *IEEE Signal Processing Mag.*, vol. 13, Nov. 1996, pp. 47-60.

[13] E. Çekli and H.A. Çirpan, "Deterministic Maximum Likelihood Approach for Localication of Near-Field Sources," *AEÜ Int'l J. of Electron. and Commun.,* vol. 56, no.1, 2002, pp. 1-10.

[14] B. Hochwald and A. Nehorai, "Concentrated Cramer-Rao Bound Expression," *IEEE Trans. on Information Theory*, vol. 40, Mar. 1994, pp. 363-371.

Jose G. Arceo-Olague received the BSc degree in communications and electronics from the Autonomous University of Zacatecas, Mexico in 2000, and the MSc from the CITEDI-IPN Research Center, Tijuana, México in 2003. He is working toward his PhD degree in communication and electronics. Actually he is an Academic Visiting Researcher at the Wireless Communications Group (WCG), CICESE Research Center in Ensenada, Mexico. His research interests are wireless communications systems, digital signal processing, and smart antennas.

David. H. Covarrubias-Rosales received the PhD in telecommunications (Cum Laude) from the Universitat Politécnica de Catalunya, Barcelona, Spain. He received the MSc in telecommunications, CICESE, México, and BSc in electronics and telecommunications engineering at the Universidad Autónoma de México, UNAM, Mexico. He has been a faculty member of the Electronics and Telecommunication Department, CICESE Research Center, Center of Scientific Research and Higher Education of Ensenada (CICESE), Ensenada, Baja California, Mexico, since June 1984. His research areas are 3G mobile communications systems and smart antennas.

Jose M. Luna-Rivera received the BS and M. Eng. in electronics engineering from the Autonomous University of San Luis Potosi, Mexico, in 1997 and 1998, respectively. He received the PhD degree in electrical engineering from the University of Edinburgh, UK, in 2003. He is currently an Associate Professor at the College of Sciences of the Autonomous University of San Luis Potosi, Mexico. His research interests focus on interference cancellation techniques for wireless communication, particularly multiuser detection, forward error correction coding, and space-time coding. He also has an interest in chaotic communications.